Histidine-rich glycoprotein inhibits HIV-1 infection in a pH-dependent manner

Ezequiel Dantas,[1] Fernando Erra Díaz,[1] Pehuén Pereyra Gerber,[1] Augusto Varese,[1] Diana Alicia Jerusalinsky,[2] Alberto L. Epstein,[3] Hernán J. García Rivello,[4] Ana del Valle Jaén,[4] Julieta B. Pandolfi,[4] Ana Ceballos,[1] Matias Ostrowski,[1] Juan Sabatté,[1*] Jorge Geffner[1*#]

[1]Instituto de Investigaciones Biomédicas en Retrovirus y SIDA (INBIRS), Universidad de Buenos Aires (UBA) and Consejo Nacional de Investigaciones Científicas y Técnicas (CONICET), Buenos Aires, Argentina.

[2]Instituto de Biología Celular y Neurociencias (IBCN), CONICET-UBA. Buenos Aires, Argentina.

[3]UMR Inserm U1179 – UVSQ, UFR des sciences de la santé, Université de Versailles Saint Quentin en Yvelines. Montigny le Bretonneux, France.

[4]Servicio de Anatomía Patológica. Hospital Italiano. Buenos Aires. Argentina.

*J.S. and J.G. contributed equally to this work.

#Address correspondence to Jorge Geffner, jorgegeffner@gmail.com.

Running head: Histidine-rich glycoprotein and HIV-1

Word counts (text): 6174

Word counts (abstract): 182

ABSTRACT

Histidine-rich glycoprotein (HRG) is an abundant plasma protein with a multidomain structure allowing its interaction with many ligands including phospholipids, plasminogen, fibrinogen, IgG antibodies, and heparan sulfate. HRG has shown to regulate different biological responses such as angiogenesis, coagulation and fibrinolysis. Here, we found that HRG almost completely abrogated the infection of GHOST, Jurkat, CD4+ T cells, and macrophages by HIV-1 at low pH (range 6.5 to 5.5) but not at neutral pH. HRG was shown to interact with heparan sulfate expressed by target cells inhibiting an early post-binding step associated to HIV-1 infection. More importantly, by acting on the viral particle itself, HRG induced a deleterious effect which reduces viral infectivity. Because cervicovaginal secretions in healthy women show low pH values, even after semen deposition, our observations suggest that HRG might represent a constitutive defence mechanism in the vaginal mucosa. Of note, low pH also enabled HRG to inhibit the infection of Hep-2 cells and Vero cells by respiratory syncytial virus (RSV) and herpes simplex virus-type 2 (HSV-2), respectively, suggesting that HRG might display a broad antiviral activity under acidic conditions. **IMPORTANCE.** Vaginal intercourse represents a high-risk route for HIV-1 transmission. The efficiency of male-to-female HIV-1 transmission has been estimated as 1 in every 1,000 episodes of sexual intercourse, reflecting a high degree of protection conferred by the genital mucosa. However, the contribution of different host factors to the protection against HIV-1 at mucosal surfaces remains poorly defined. Here, we report for the first time that acidic values of pH enable the plasma protein histidine-rich glycoprotein (HRG) to strongly inhibit HIV-1 infection. Because cervicovaginal secretions usually show low pH values, our observations suggest that HRG might represent a constitutive antiviral

mechanism in the vaginal mucosa. Interestingly, infection by other viruses such as respiratory syncytial virus and herpes simplex virus-type 2 was also markedly inhibited by HRG at low pH values, suggesting that extracellular acidosis enables HRG to display a broad antiviral activity.

50 **Introduction**

51 Histidine rich glycoprotein (HRG) is a 75 kDa single polypeptide chain protein produced
52 by the liver (1), found at relatively high concentrations (~ 150 µg/ml) in human plasma (2,
53 3). It has a multi-domain structure (4) enabling its interaction with a variety of ligands such
54 as phospholipids (5), plasminogen (6), fibrinogen (7), Zn^{2+} (8), and heparan sulfate (HS)
55 (9). HRG has been shown to modulate different biological processes including
56 angiogenesis, cell adhesion, coagulation, and fibrinolysis (2, 10).

57

58 Due to the unusually high content of histidine residues (pKa ~ 6.5) which account for 13%
59 of its total amino acids content (11), HRG acquires a positive net charge upon exposure to
60 acidic environments (4). In fact, it has been proposed that HRG acts as a pH sensor, by
61 recognizing negatively charged glycosaminoglycans (GAGs) such as HS, dermatan sulfate
62 and chondroitin sulfate in a pH-dependent mode (12). This property of HRG might be
63 particularly relevant in the scenario of HIV-1 infection. Heparan sulfate has shown to play
64 an important role in sexual transmission of HIV-1 by acting as an attachment factor which
65 contributes to the binding of the virus to vaginal epithelial cells, CD4+ T cells and
66 macrophages (13). Moreover, it is well established that semen, the major vector of HIV-1
67 transmission, shifts the pH of the vaginal secretions from strong acidic values (pH range
68 3.5-5.5) (14-16) to values ranged from 6.0 to 7.0 for several hours after sexual intercourse
69 (17, 18). Thus, we hypothesized that HRG might inhibit HIV-1 infection by preventing the
70 interaction of HIV-1 with HS in the scenario of male to female sexual transmission of HIV-
71 1.

In this study, using different target cells and viral sources, we found that HRG almost completely abrogated HIV-1 infection at low pH values (pH range 6.5 to 5.5). We also show that the antiviral activity of HRG was not restricted to HIV-1; it effectively inhibited the infection mediated by other enveloped virus such as respiratory syncytial virus (RSV) and herpes simplex virus-type 2 (HSV-2), suggesting that HRG might display a broad antiviral activity at low pH.

RESULTS

HRG strongly inhibits HIV-1 infection at low pH.

We first analyzed whether HRG was able to modulate GHOST cell infection by HIV-1. In these experiments, we used GHOST cells stably transfected with CD4, CXCR4 and CCR5 genes, containing a green fluorescent protein (GFP) gene under the control of a HIV-2 long terminal repeat. Cells were exposed to HIV-1 (X4 HIV-1_{IIIB} or R5 HIV-1_{BAL}) for 90 min at 37ºC at different pH values, in the absence or presence of HRG (125 µg/ml), washed and cultured for 48 h at pH 7.3. Infection was then revealed by flow cytometry. Exposure to acidic pH values (6.5, 6.0 and 5.5) enabled HRG to strongly inhibit GHOST cell infection (**Figure 1A-C**), even when used at concentrations as low as 25 µg/ml (**Figure 1D**). No inhibition of infection was observed in cells exposed to low pH values, in the absence of HRG (**Figure 1A-C**). A similar inhibitory effect was found when the CD4+ T cell line Jurkat was challenged with a GFP-encoding NL4-3 virus using either, plasma purified HRG (**Figure 1E and G)** or recombinant HRG (**Figure 1F**). We then analyzed the antiviral effect mediated by HRG using macrophages and primary CD4+ T cells. Macrophages were obtained from monocytes isolated from peripheral blood (% purity >94%) and cultured for 5 days with GM-CSF, while CD4+ T cells were isolated from peripheral blood mononuclear cells (PBMCs) by negative selection (% purity > 95%). Macrophages were challenged with HIV-1_{BAL} at different pH values for 90 min at 37°C, in the absence or presence of HRG. After washing, cells were cultured for 10 days at pH 7.3, and the percentage of infected cells was determined by intracellular staining of p24 using the mAb Kc-57. Consistent with the results observed in GHOST and Jurkat cells, we found that HRG strongly inhibited HIV-1 infection in macrophages challenged at low pH (**Figure**

1H). A similar inhibitory effect was found in activated-CD4+ T cells challenged with a GFP-encoding NL4-3 virus (**Figure 1I**). To confirm that inhibition of HIV-1 infection was not related to diminished cell viability induced by HRG at low pH, cell viability assays were performed. These experiments were carried out in GHOST cells, Jurkat cells, macrophages, and primary activated CD4+ T cells under similar experimental conditions than those employed in the infections assays described in **Figure 1**, in the absence of HIV-1. Using both, an annexin-FITC/propidium iodide staining kit and a MTS assay, we found that cell exposure to low pH in the absence or presence of HRG did not compromise cell viability effect (data not shown). We conclude that extracellular acidosis enables HRG to strongly inhibit HIV-1 infection.

HRG is expressed in the female reproductive tract and binds to epithelial cells, CD4+ T lymphocytes and macrophages in a pH-dependent manner.

HRG is produced by the liver and it can be found at high concentrations (~ 150 µg/ml) in plasma. Because the tissue distribution of HRG remains largely unknown and considering that most HIV-1 transmission occurs through mucosal surfaces, we analyzed the expression of HRG at the human female reproductive tract. The squamocolumnar junction of the cervix, the ectocervix and the vagina showed an intense staining for HRG in the basal/parabasal cell layers of the epithelium. The anal canal mucosa also exhibited a high expression of HRG and as expected, a diffuse cytoplasmic staining was observed in the liver, the main source of plasma HRG (**Figure 2A**). These observations indicate that HRG is present at the two most frequent entry portals of HIV-1. The early attachment of HIV-1

to genital epithelial cells and CD4+ target cells is mediated by a variety of cell-surface molecules, including HS (19, 20). Previous studies performed by resonant mirror biosensor techniques have shown that HRG binding to immobilized HS is pH-sensitive, showing a maximum between 5.7 and 6.1 (12). Consistent with these observations, we found that HRG binding to the ectocervical epithelial cell line Ect1/E6E7 (**Figure 2B**), CD4+ T lymphocytes and macrophages (**Figure 2C)** showed a very strong pH-dependence; binding was negligible at pH 7.3, but markedly increased at low pH (5.5-6.5). As expected, the enhanced binding of HRG to CD4+ T cells and macrophages induced by low pH was completely prevented by heparin (**Figure 2C)**.

Low pH enables HRG to inhibit early cellular events associated with HIV-1 infection. The stratified squamous epithelium that lines the vagina and ectocervix represents an important physical barrier to incoming HIV-1(21). These cells are not susceptible to HIV-1 infection but are able to bind viral particles promoting the trans-infection of CD4+ T cells and macrophages (22-24). Using the ectocervical epithelial cell line Ect1/E6E7 and the vaginal epithelial cell line VK2/E6E7, we analyzed whether HRG was capable of inhibiting early cellular events associated to the interaction between HIV-1 and genital epithelial cells. In these experiments, cells were incubated for 90 min at 37ºC at different pH values, in the absence or presence of HRG. Then, cells were extensively washed, lysed, and cell-associated HIV-1 was analyzed by a p24 ELISA. Results in **Figure 3A** and **B** showed that the amount of cell-associated p24 antigen was lower in Ect1 and VK2 cells treated with HRG at low pH but not at neutral pH. Similar observations were made in cells permissive to HIV-1 infection such as activated CD4+ T cells, macrophages, Jurkat and GHOST cells (**Figure 3C-F**).

In order to determine whether this inhibitory effect was due to the inhibition of HIV-1 binding to the cell surface, additional experiments were performed by incubating Jurkat cells for 90 min at 4°C, instead of 37ºC, in the absence or presence of HRG. Surprisingly, no inhibition of HIV-1 binding was observed (**Figure 3G**), suggesting that low pH enables HRG to inhibit early cellular events associated to HIV-1 infection after viral binding to the cell surface.

HRG compromises viral infectivity at low pH.

The results described above suggested that the inhibition of early cellular events associated to HIV-1 infection induced by HRG at low pH was dependent on the interaction of HRG with cell-associated HS. To confirm this presumption we performed additional experiments in cells lacking HS expression. GHOST cells were cultured for three days in sulfate free medium supplemented with sodium chlorate, an inhibitor of sulfation (25). Alternatively, cells were treated with heparinases I, II, and III. The results obtained (**Figure 4A and B**) showed that cells cultured under these conditions markedly reduced not only the expression of HS (**Figure 4A**), but also the enhanced binding of HRG to the cell surface observed at pH 6.0 (**Figure 4B**). As expected, HRG failed to inhibit the early association of HIV-1 with heparinase-treated Jurkat cells (**Figure 4C**), but surprisingly it was still capable of markedly inhibiting HIV-1 infection in Jurkat and GHOST cells lacking HS (**Figure 4D-F**). Considering that only a marginal binding of HRG was observed in target cells lacking HS, we hypothesized that the antiviral effect mediated by HRG might involve a direct action exerted on the viral particle itself. To analyze this hypothesis, HIV-1 particles were pretreated with HRG for 1 h at pH 7.3 or 6.0. Then, HRG was washed out by

ultracentrifugation and the virus was exposed to Jurkat cells, at pH 7.3 or 6.0, respectively. The results obtained showed that pretreatment of the virus with HRG at either pH 7.3 or 6.0 did not exert any effect on the binding of HIV-1 to Jurkat cells (**Figure 4G**). By contrast, pretreatment of the virus with HRG at pH 6.0 markedly prevented the infection of Jurkat cells (**Figure 4H**), suggesting that low pH enables HRG to induce a deleterious effect on the viral particle.

HRG interacts with HIV-1 at low pH.

To analyze whether low pH values actually enabled HRG to interact with the viral particles, we performed a new set of experiments using HRG-coated beads and HIV-1 carrying Gag-associated GFP (HIV NL4-3 Gag-iGFP). Validating this experimental approach, we observed that HRG efficiently bound to latex beads (**Figure 5A left**), and also that beads coated with the mAb 2G12 directed to gp120, but not BSA or non-specific IgG, similarly attached fluorescently labeled HIV-1 particles, at pH 7.3 and 6.0 (**Figure 5A, right**). We then analyzed the influence exerted by low pH on the interaction of HRG with HIV-1, and found that beads coated with plasma purified or recombinant HRG, but not with BSA or unspecific IgG, efficiently captured HIV-1 particles at low pH. We also found that heparin completely prevented HIV-1 capture by HRG-coated beads, suggesting that it involves the interaction of HRG with anionic molecules expressed on the virus surface. Interestingly, the enhanced binding of HIV-1 to HRG-coated beads observed at low pH was shown to be a reversible phenomenon. In fact, upon pH neutralization, the viral particles detached from HRG-coated beads (**Figure 5B and C**).

HRG exerts an irreversible deleterious effect on the viral particles.

Having shown that low pH enables HRG to efficiently interact with the viral surface, we then analyzed whether this interaction resulted in an irreversible loss of virus infectivity. In these experiments, HIV-1 was exposed to HRG at pH 7.3 or 6.0 for 90 min at 37°C. After this period, the viral suspension cultured with HRG at pH 6.0 was neutralized back to pH 7.3. Pretreatment of HIV-1 with HRG at low pH values for 90 min did not affect the binding of virus particles to Jurkat cells (**Figure 6A**) but markedly reduced virus infectivity (**Figure 6B**). Interestingly, the antiviral effect induced by HRG was not reversed when the viral particles that had been preincubated with HRG at pH 6.0 for 90 min were further incubated for 90 or 180 min at pH 7.3, before infecting Jurkat cells. On the contrary, a progressive loss of infectivity was observed (**Figure 6C**).

HRG displays a broad antiviral activity at low pH.

We then analyzed whether low pH might enable HRG to display a broad antiviral activity. Vesicular stomatitis virus (VSV)-G pseudotyped lentivirus, represent powerful tools to study virus entry and infection in a variety of target cells due to their broad tropism (26). We first determined whether HRG inhibited the infection of Jurkat cells by VSV-G-pseudotyped HIV-1 lacking gp120. HRG did not exert any inhibitory effect at pH 7.3, but markedly inhibited infection at pH values of 6.5, 6.0 and 5.5 (**Fig. 7A**). We also studied the effect of HRG on the infection mediated by respiratory syncytial virus (RSV). **Figure 7B** shows that low pH enabled HRG to prevent the infection of the epithelial cell line Hep 2 by RSV. Results depicted in **Figure 7C,** on the other hand, show that HRG also inhibited Vero cell infection by herpes simplex virus type 2 (HSV-2) at low pH values, although the inhibition was less pronounced compared with the observations made for HIV-1-infected cells. A strong inhibitory effect was also observed when the ectocervical epithelial cell line

234 Ect1/E6E7, the vaginal epithelial cell line VK2/E6E7, and the epitheloid cervix carcinoma
235 cell line HeLa were challenged with an HSV-1 derived amplicon vector encoding GFP (27)
236 (**Figure 7D-F**). Of note, results in **Figure 7D and E** show that HRG strongly inhibited the
237 infection of ECT-1 and VK-2 cells at pH 7.3, suggesting that HRG might display an
238 antiviral activity against certain virus not only at acidic values of pH, but also under neutral
239 pH values.
240
241 **DISCUSSION**
242
243 No previous studies have analyzed whether HRG might be able to exert any antiviral
244 activity. Here we demonstrate that HRG strongly inhibits HIV-1 infection at low pH. HRG
245 was shown to interact with cell HS in a pH-dependent manner, inhibiting the early
246 association of HIV-1 with target cells. The fact that inhibition was observed at 37°C but not
247 at 4°C, suggests that HRG inhibits a post-binding step such as virus fusion or endocytosis.
248 Moreover, by interacting with the viral particle, HRG induced a deleterious effect which
249 resulted in the loss of viral infectivity. Interestingly, HRG also efficiently inhibited the
250 infection mediated by RSV and HSV-2 in cells challenged at low pH, suggesting that HRG
251 might display a broad antiviral activity.
252 Previous studies have shown that low pH enables HRG to mediate cytotoxic effects against
253 fungi and bacteria (28-30). In this regard, it has been reported that HRG binds to *Candida*
254 *spp.* inducing breaks in the cell wall and that low pH (pH 5.5) increases the membrane-
255 disrupting activitiy of HRG (29). The same authors showed that HRG preferentially lysed
256 ergosterol-containing liposomes but not cholesterol-containing ones, suggesting that the
257 cytotoxic effect induced by HRG might be preferentially induced on fungal but not on other

eukaryotic membranes (29). Another study from the same laboratory showed that HRG induced the lysis of the Gram-positive bacteria *Enterococcus faecalis* at pH 5.5, being this cytotoxic effect fully prevented by heparin (28).

These microbicidal actions exerted by HRG at low pH resemble those elicited by either natural or synthetic histidine-rich peptides (31). In contrast to cationic antimicrobial peptides, histidine-rich peptides exert a bactericidal and fungicidal activity at low pH, but not at neutral pH (31). Histidines (pKa ~ 6.5) are largely unprotonated and uncharged at neutral pH, but become protonated and positively charged at low pH. This change promotes the interaction of histidine-rich peptides with anionic lipids expressed on the surface of bacteria and fungi, thereby inducing membrane destabilization and permeabilization (29, 30). The fact that bacterial and fungal membranes, but not mammalian membranes are enriched in anionic phospholipids, could explain why histidine-rich peptides are cytotoxic to bacteria and fungi (32, 33), but not to mammalian cells. Interestingly, in spite that lipids of enveloped virus are derived from the host membranes from which budding occurs, studies directed to characterize the overall lipid composition of HIV-1 particles and plasma membranes of producer cells revealed and enrichment of cholesterol and sphingomyelin in the virus (34, 35). Moreover, mature virions express phosphatidylserine (PS) and phosphatidylethanolamine (PE) on their external surface, indicating that virus membrane does not retain the asymmetric lipid distribution of host producer cells (35). These differences could explain why HRG exerts a deleterious effect on viral particles but not on target cells. A limitation of our study is that the association of HRG with HIV-1 and the subsequent loss of viral infectivity were only analyzed in viruses produced by 293T cells, and not in those produced by T cells or macrophages, which might differ in both, the host

282 cell factors expressed at the viral surface and its ability to bind HRG. Further studies are
283 needed to determine whether a similar mechanism accounts for the inhibition of HIV-1
284 infection mediated by HRG in CD4+ T cells and macrophages.
285
286 Interestingly, not only low pH but also Zn^{2+} is able to impose a positive charge to the
287 histidine-rich domain of HRG (1, 8). In fact, the ability of HRG to interact with cell-
288 surface-HS at neutral pH markedly increases following the interaction of HRG with Zn^{2+}, at
289 physiological concentrations of Zn^{2+} (~10-20 μM) (9). We speculate that Zn^{2+} might enable
290 HRG to exert an antiviral effect at neutral pH. This hypothesis, however, should be
291 rigorously tested because most of Zn^{2+} is tightly bound to plasma proteins reducing free
292 Zn^{2+} concentrations from micromolar to nanomolar levels (36). Interestingly, it has been
293 previously described that HRG can be found in platelet´s granules along with high
294 concentrations of Zn^{2+}(37). Since platelets exert antiviral effects (38, 39), we surmise that
295 platelet´s activation and degranulation might enable HRG to inhibit viral infections in a
296 Zn^{2+}-dependent mode. Further studies are required to test this possibility.
297
298 We also found that low pH enhanced the binding of HIV-1 to the epithelial cell lines Ect1
299 and VK2. Interestingly, we have previously reported that HIV-1 binding to spermatozoa,
300 but no to CD4+ T cells or dendritic cells, was markedly increased at pH 6.0 or pH 6.5,
301 compared with neutral pH (40). Because HS plays a major role in the binding of HIV-1 to
302 epithelial cells (20) we surmise that low pH might increase the affinity of the envelope
303 glycoprotein gp120 or any of the host-derived proteins which are incorporated to the virus
304 during the budding process(41, 42) to HS via protonation of histidine residues. In fact, low

pH values in the range 6.0-7.0 have shown to increase the binding of a number of proteins such as the gp64 of baculovirus, prion protein, selenoprotein P, GM-CSF, VEGF, and the non-fibrillar form of beta-amyloid peptide to HS via protonation of histidine residues (43, 44). Further studies are required to test this hypothesis.

No previous studies have analyzed the presence and the role of HRG at mucosal surfaces, the first entry portals for many infectious agents. We found that HRG is present in the basal/parabasal cell layers of the ectocervix and vaginal epithelium, as well as in the anal canal mucosa. Whether or not this reflects a local production of HRG remains to be determined. Besides this, considering the high concentrations of plasma HRG (~ 150 μg/ml) we speculate that microabrasions of the mucosal surface induced either by genital ulcer diseases or mechanical stress during intercourse might contribute to increase the local concentration of HRG. It is of note that this is not an unusual scenario; in fact, epithelial microabrasions of the vaginal mucosa are usually detected in 60% of healthy women after consensual intercourse (45). A limitation of our study is the lack of data proving that the HRG concentration present at the cervicovaginal tissues is capable of exerting its anti-viral effect in vivo. Further studies in HRG knockout mice are required to assess this.

These observations places HRG at the female reproductive tract and since the cervicovaginal fluids in healthy women show low pH values (14, 15), even after semen deposition (17, 18, 46), we surmise that HRG might exert a protective role against sexually transmitted virus such as HIV-1. It should be emphasized that the antiviral activity of the HRG might not be limited to the female reproductive tract since mucosal surfaces from other tissues such as the urinary, the gastrointestinal and the respiratory tracts, are usually

exposed to low pH values too (14, 47-49). Different studies have shown that, even in the absence of inflammatory processes, the pH of the airway surface liquid (ASL), a thin (~25 µm) layer of fluid that coats the airway mucosal surface, is acidic due to a constitutive and amiloride-sensitive process of proton secretion by the airway epithelium, which is further activated during airway inflammation (50, 51). The intraluminal pH gradient along the gastrointestinal tract shows acidic pH values in the small intestine (pH 6.0–7.4) and the caecum (pH 5.7) (52-54). Not only mucosal surfaces, but also the skin surface is acidic in a range from pH 4.0 to 6.0 (55). This acid mantle strongly contributes to the barrier function of the skin by preventing infection by bacteria, fungi, and virus (56). Furthermore, is even possible that HRG could exert an antiviral activity at neutral pH since the infection of the vaginal and ectocervical epithelial cell lines VK2/E6E7 and Ect1/E6E7 by an HSV-1 derived amplicon was markedly inhibited not only at low pH, but also at neutral pH. Further studies are required to determine the relevance of this observation as well as the mechanisms through which HRG might display an antiviral activity at neutral pH values. Together, our observations suggest that HRG might display an antiviral activity at the major portals of entry for infectious pathogens.

MATERIALS AND METHODS

Ethics statement. The institutional review board of the "Hospital Italiano" (Buenos Aires, Argentina) approved the study. All blood donors provided written informed consent.

HRG purification. HRG was purified from healthy plasma donors ("Hospital Mendez", Buenos Aires, Argentina), as previously described (57). Briefly, human plasma was loaded into chromatography columns containing Ni-NTA agarose (Qiagen) and incubated at 4°C in agitation for 1 h. After plasma elution, weakly bound contaminant material was removed with a series of increasing imidazole concentrations; 5 mM, 20 mM and 100 mM in TBS, pH 8,0. HRG was then eluted with a 250 mM imidazole solution, extensively dialyzed against PBS and frozen at -80°C. HRG concentration was assessed by ELISA (Sino Biological).

Cells, plasmids and viral stocks. PBMCs were isolated from healthy volunteers ("Hospital Mendez", Buenos Aires, Argentina), by standard density gradient centrifugation on Ficoll-Hypaque. Monocytes were obtained using CD14 microbeads (Miltenyi Biotec). The purity was checked by FACS analysis using a mAb directed to CD14 and was found to be >94%. To obtain macrophages, monocytes were suspended in RPMI 1640 medium (GIBCO) and adhered for 1 h to flat-bottom 24-multiwell plates, afterwards cells were cultured in medium supplemented with 10% fetal bovine serum (GIBCO) and 40ng/ml of GM-CSF (Miltenyi Biotec) for 6 days. CD4+ T cells were isolated from PBMCs by negative selection, using a CD4 + T-cell Isolation Kit (Miltenyi Biotec) (purity > 95%). Cells were activated for 3 days with anti-CD3/CD28 beads (Miltenyi Biotec) in 10 U/ml of IL-2 supplemented culture medium.

370 The osteosarcoma cell line GHOST, stably transfected with CD4, CXCR4 and CCR5 genes
371 and cotransfected with the HIV-2 long terminal repeat driving a EGFP construct which
372 transcribes upon HIV-1 DNA integration with the cellular DNA, was obtained from the
373 AIDS Reagent Program, Division of AIDS, NIAID, NIH. The clone E6-1 of the human
374 CD4+ T cell line Jurkat, the neoplastic cell line H9 infected by HIV-1_{IIIB}, the HIV-1_{BaL}
375 strain and the HIV-1 vector plasmid pNL4-3, were obtained from the AIDS Reagent
376 Program. The HIV-1 pUC-NL4-3 Gag internal GFP was obtained from Michael Schindler
377 (Institute of Virology, Munich, Germany). The pCMV-VSV-G was obtained from Addgene
378 (Sydney, Australia). The pBR-NL4.3-IRES-eGFP-nef+ encoding full-length HIV-1 in the
379 pBR322 backbone under the control of viral long terminal repeat promoter was kindly
380 provided by F. Kirchhoff (Institute of Molecular Virology, Ulm University Medical Center,
381 Ulm, Germany).
382
383 Vero, VK2/E6E7, Ect1/E6E7, and HEp-2 cells were purchased from ATCC and cultured
384 according to the manufacturer's instructions. HIV-1 NL4-3, HIV-1 NL4-3-EGFP, HIV-1
385 NL4-3 Gag-iGFP and the VSV-G pseudotyped ΔEnv-EGFP NL4-3 viral stocks were
386 obtained transfecting HEK 293T cells, as previously described (58, 59). The HIV-1_{IIIB} viral
387 stock was obtained from H9 supernatants, as previously described (60). The HIV-1_{Bal} strain
388 was amplified in monocyte-derived macrophages. In all cases, cell supernatants were
389 filtered through a 0.45-micron filter and concentrated by ultracentrifugation at 28 000 rpm
390 for 90 min at 4°C (L7-65 ultracentrifuge; Beckman Coulter). The G-strain of HSV-2 was a
391 gift from C. Pujol (University of Buenos Aires, Argentina). HSV-2 was propagated and
392 titrated in Vero cells as described previously (61), and the infectious titer was expressed as

plaque forming units (pfu) per ml. The HSV-1 derived amplicon vector encoding GFP was kindly provided by D. Jerusalinsky (University of Buenos Aires, Argentina) and A. L. Epstein (Université Claude Bernard Lyon, Villeurbanne, France). The RSV subtype A, strain Long was a kind gift from Elsa Baumeister (Malbrán Institute, Argentina).

Infection assays. Infection of CD4+CXCR4+CCR5+GHOST cells was performed as described (4). Briefly, 12000 GHOST cells were plated in 24 flat-bottom multiwell plates, in a final volume of 400 µl/well (RPMI medium supplemented with 10% fetal calf serum) on day 0. The next day, cells were washed and challenged with HIV-1 (X4 HIV-1_{IIIB} or R5 HIV-1_{BAL}, 10 ng of p24/well) for 90 min at 37ºC, in the absence or presence of HRG (125 µg/ml), at different pH values. After 90 min of incubation at 37ºC, cells were washed and cultured at pH 7.3 for 72 h. Then, infection was analyzed by flow cytometry. Jurkat cells and anti-CD3/CD28 activated CD4+ T cells were incubated in 96 U-bottom well plates at concentrations or 30000 cells/well/100 µl and 100000 cells/well/100 µl, respectively. Jurkat and CD4+ T cells were challenged with X4 HIV-1 NL4-3 EGFP virus (10ng p24/well and 50ng p24/well, respectively) for 90 min at 37°C, in the absence or presence of HRG (125 µg/ml), at different pH values. Then, cells were washed, cultured for 3 or 5 days at pH 7.3, and infection was revealed by flow cytometry. Macrophages were cultured in 24 flat-bottom multiwell plates (350000 cells/well/350 µl) and infected with HIV-1_{BAL} (50ng p24/well) at different pH values, in the absence or presence of HRG (125 µg/ml), for 90 min at 37°C. After washing with culture medium, macrophages were cultured for 10 days at pH 7.3, and the percentage of infected cells was determined by intracellular staining of p24 with the mAb Kc-57 (Beckman-Coulter). Vero cells were plated to 80% confluence in 24 flat-bottom multiwell plates, and challenged with a pre-titered amount of HSV-2 for 90

min at 37ºC, in the absence or presence of HRG (125 µg/ml), at different pH values. Then, cells were washed with PBS twice and cultured at pH 7.3 for 72 h at 37°C. Infection was evaluated by determining the number of pfu/well. Ect1/E6E7, VK2/E6E7 and HeLa cells were plated to 80% confluence in flat-bottom 24 multiwells plates and challenged with a pre-titered amount of HSV-1 derived amplicon vector encoding GFP, in the presence or absence of HRG (125 µg/ml), for 90 min at 37°C, at different pH values. Then, cells were washed with PBS twice and cultured at pH 7.3, for 72 h at 37°C. Cells were harvested and analyzed by flow cytometry. HEp-2 cells (50% confluence) were challenged with RSV (MOI 0.5), in the presence or absence of HRG (125 µg/ml), for 90 min at 37°C, at different pH values. Cells were then washed twice and cultured for at pH 7.3 for 3 days in 48-well plates in culture medium supplemented with 2% FCS. Next, cells were harvested, and the expression of viral antigen was detected by intracellular staining and flow cytometry, using a mouse anti-human RSV mAb (EMD Millipore Corporation) and a PE-goat anti-mouse-IgG (Dako).

Cell viability assays. Apoptosis and necrosis was evaluated by staining with annexin-FITC/propidium iodide (BD Biosciences) and flow cytometry. Cells were labeled with annexin-V FITC and propidium iodide for 15 min at room temperature and analyzed by flow cytometry using a BD FACSCanto cytometer and BD FACSDiva software (BD Biosciences). Cell viability was also assessed by using the MTS assay (Abcam), based on the reduction of the MTS tetrazolium by viable cells, as described by the manufacturer.

HRG binding to target cells. Ect1/E6E7 cells, CD4+ T cells and macrophages, were incubated at 4°C for 1 h, in the absence or presence of different concentrations of HRG, at pH values of 7.3, 6.5, 6.0, or 5.5. After washing, bound HRG was revealed by flow cytometry using a mouse mAb anti-HRG (Sino Biological), and an Alexa-488 anti mouse mAb (Jackson Immuno Research).

HIV-1 attachment to target cells. The cell lines Ect1/E6E7, VK2/E6E7, Jurkat, GHOST, activated-CD4+ T cells and macrophages were incubated with HIV-1_{IIIB} or HIV-1 NL4-3 (50ng of p24/well), for 90 min at 37°C with HRG (125 µg/ml) at different pH values. In all cases, cells were washed 5 times with PBS, lysed using RIPA lysis buffer and the amount of p24 was evaluated as absorbance at 450 nm, using Genscreen ULTRA HIV Ag-Ab (Bio-Rad).

Heparan sulfate removal from target cells. To abrogate HS synthesis, GHOST cells where cultured for 36 h with 25 mM of sodium chlorate in a custom made DMEM medium lacking sulfate, supplemented with 10% of fetal calf serum, as described (25). For enzymatic removal of HS, Jurkat and GHOST cells were treated with 5 mIU/ml of a heparinase I and III blend (Sigma) and 5 mIU/ml of heparinase II (Sigma), for 1h at 37°C.

HRG binding to HIV-1. Aldehyde/Sulfate Latex beads (Molecular Probes) were coated with purified HRG, recombinant HRG (Sino Biological), bovine serum albumin (Sigma-Aldrich), human IgG (Sigma-Aldrich) or the anti-gp120 mAb 2G12 (AIDS Reagent Program), following the manufacturer's instructions. Briefly, 70 µg of each protein, previously dialyzed against MES buffer 0.025 M, pH 6, were added to $1x10^8$ beads that had

already been washed and suspended in MES buffer. After overnight incubation under rotation at room temperature, beads were extensively washed with a PBS-BSA 2 % solution and stored at 4°C in PBS with 0,1% glycine and 0,1% sodium azide. HIV-1 capture assays were performed as follows. 1500-2000 beads were incubated with the HIV-1 NL4-3 Gag-iGFP virus (10 ng of p24), at different pH values, at 37°C for 45min under agitation. Then, the attachment of GFP-virus to latex beads was evaluated by flow cytometry.

Immunohistochemistry. Paraffin blocks of human liver, cervix, vagina and anus were retrieved from the surgical archives of the Pathology Department of the Italian Hospital, Buenos Aires, Argentina. Paraffin immunohistochemistry was performed using a monoclonal anti-HRG antibody (Sino Biological) at 1:75 dilution. Briefly, four-micron thick sections of paraffin-embedded tissue blocks were baked for at least 30 min in an oven at 60°C. Deparaffinization, antigen retrieval, blockage of endogenous peroxidase activity, peroxidase–labeled anti-mouse IgG dispense and incubation steps were all performed on automated XT Benchmark Instrument (Ventana, Tucson, AZ, USA). Next, the slides were removed from the instrument after completion of the run, dipped 10–15 times in water to remove the oil, rinsed in tap water, dehydrated using a graded series of reagent alcohols, dipped in xylene and coverslipped for microscopic examination.

Statistics. Data are shown as mean values ± SEM. Student paired t-test was used to determine the significance of differences between treatment groups. Multiple analyses were followed by Bonferroni's multiple-comparison posttest. The p values <0.05 were considered statistically significant.

FUNDING

This work was supported by grants from the National Agency for Scientific and Technical Promotion [PICT 2014-1689 to JG] and Universidad de Buenos Aires [20020130100446BA to JG], Buenos Aires, Argentina.

ACKNOWLEDGEMENTS

We thank María Esther Dorado and Fernanda Visconti for their technical assistance.

REFERENCES

1. Priebatsch KM, Kvansakul M, Poon IK, Hulett MD. 2017. Functional Regulation of the Plasma Protein Histidine-Rich Glycoprotein by Zn2+ in Settings of Tissue Injury. Biomolecules 7.
2. Poon IK, Patel KK, Davis DS, Parish CR, Hulett MD. 2011. Histidine-rich glycoprotein: the Swiss Army knife of mammalian plasma. Blood 117:2093-101.
3. Corrigan JJ, Jr., Jeter MA, Bruck D, Feinberg WM. 1990. Histidine-rich glycoprotein levels in children: the effect of age. Thromb Res 59:681-6.
4. Borza DB, Tatum FM, Morgan WT. 1996. Domain structure and conformation of histidine-proline-rich glycoprotein. Biochemistry 35:1925-34.
5. Poon IK, Hulett MD, Parish CR. 2010. Histidine-rich glycoprotein is a novel plasma pattern recognition molecule that recruits IgG to facilitate necrotic cell clearance via FcgammaRI on phagocytes. Blood 115:2473-82.
6. Lijnen HR, Hoylaerts M, Collen D. 1980. Isolation and characterization of a human plasma protein with affinity for the lysine binding sites in plasminogen. Role in the regulation of fibrinolysis and identification as histidine-rich glycoprotein. J Biol Chem 255:10214-22.
7. Leung LL. 1986. Interaction of histidine-rich glycoprotein with fibrinogen and fibrin. J Clin Invest 77:1305-11.
8. Morgan WT. 1981. Interactions of the histidine-rich glycoprotein of serum with metals. Biochemistry 20:1054-61.
9. Jones AL, Hulett MD, Parish CR. 2004. Histidine-rich glycoprotein binds to cell-surface heparan sulfate via its N-terminal domain following Zn2+ chelation. J Biol Chem 279:30114-22.
10. Wakabayashi S. 2013. New insights into the functions of histidine-rich glycoprotein. Int Rev Cell Mol Biol 304:467-93.
11. Haupt H, Heimburger N. 1972. [Human serum proteins with high affinity for carboxymethylcellulose. I. Isolation of lysozyme, C1q and 2 hitherto unknown -globulins]. Hoppe Seylers Z Physiol Chem 353:1125-32.
12. Borza DB, Morgan WT. 1998. Histidine-proline-rich glycoprotein as a plasma pH sensor. Modulation of its interaction with glycosaminoglycans by ph and metals. J Biol Chem 273:5493-9.
13. Bartlett AH, Park PW. 2010. Proteoglycans in host-pathogen interactions: molecular mechanisms and therapeutic implications. Expert Rev Mol Med 12:e5.
14. Garcia-Closas M, Herrero R, Bratti C, Hildesheim A, Sherman ME, Morera LA, Schiffman M. 1999. Epidemiologic determinants of vaginal pH. Am J Obstet Gynecol 180:1060-6.

15. Thinkhamrop J, Lumbiganon P, Thongkrajai P, Chongsomchai C, Pakarasang M. 1999. Vaginal fluid pH as a screening test for vaginitis. Int J Gynaecol Obstet 66:143-8.
16. O'Hanlon DE, Moench TR, Cone RA. 2013. Vaginal pH and microbicidal lactic acid when lactobacilli dominate the microbiota. PLoS One 8:e80074.
17. Bouvet JP, Gresenguet G, Belec L. 1997. Vaginal pH neutralization by semen as a cofactor of HIV transmission. Clin Microbiol Infect 3:19-23.
18. Tevi-Benissan C, Belec L, Levy M, Schneider-Fauveau V, Si Mohamed A, Hallouin MC, Matta M, Gresenguet G. 1997. In vivo semen-associated pH neutralization of cervicovaginal secretions. Clin Diagn Lab Immunol 4:367-74.
19. Patel M, Yanagishita M, Roderiquez G, Bou-Habib DC, Oravecz T, Hascall VC, Norcross MA. 1993. Cell-surface heparan sulfate proteoglycan mediates HIV-1 infection of T-cell lines. AIDS Res Hum Retroviruses 9:167-74.
20. Connell BJ, Lortat-Jacob H. 2013. Human immunodeficiency virus and heparan sulfate: from attachment to entry inhibition. Front Immunol 4:385.
21. Burgener A, McGowan I, Klatt NR. 2015. HIV and mucosal barrier interactions: consequences for transmission and pathogenesis. Curr Opin Immunol 36:22-30.
22. Wu Z, Chen Z, Phillips DM. 2003. Human genital epithelial cells capture cell-free human immunodeficiency virus type 1 and transmit the virus to CD4+ Cells: implications for mechanisms of sexual transmission. J Infect Dis 188:1473-82.
23. Kohli A, Islam A, Moyes DL, Murciano C, Shen C, Challacombe SJ, Naglik JR. 2014. Oral and vaginal epithelial cell lines bind and transfer cell-free infectious HIV-1 to permissive cells but are not productively infected. PLoS One 9:e98077.
24. Bobardt MD, Saphire AC, Hung HC, Yu X, Van der Schueren B, Zhang Z, David G, Gallay PA. 2003. Syndecan captures, protects, and transmits HIV to T lymphocytes. Immunity 18:27-39.
25. Baeuerle PA, Huttner WB. 1986. Chlorate--a potent inhibitor of protein sulfation in intact cells. Biochem Biophys Res Commun 141:870-7.
26. Tani H, Morikawa S, Matsuura Y. 2011. Development and Applications of VSV Vectors Based on Cell Tropism. Front Microbiol 2:272.
27. Melendez ME, Fraefel C, Epstein AL. 2014. Herpes simplex virus type 1 (HSV-1)-derived amplicon vectors. Methods Mol Biol 1144:81-98.
28. Rydengard V, Olsson AK, Morgelin M, Schmidtchen A. 2007. Histidine-rich glycoprotein exerts antibacterial activity. FEBS J 274:377-89.
29. Rydengard V, Shannon O, Lundqvist K, Kacprzyk L, Chalupka A, Olsson AK, Morgelin M, Jahnen-Dechent W, Malmsten M, Schmidtchen A. 2008. Histidine-rich glycoprotein protects from systemic Candida infection. PLoS Pathog 4:e1000116.
30. Shannon O, Rydengard V, Schmidtchen A, Morgelin M, Alm P, Sorensen OE, Bjorck L. 2010. Histidine-rich glycoprotein promotes bacterial entrapment in clots and decreases mortality in a mouse model of sepsis. Blood 116:2365-72.
31. Kacprzyk L, Rydengard V, Morgelin M, Davoudi M, Pasupuleti M, Malmsten M, Schmidtchen A. 2007. Antimicrobial activity of histidine-rich peptides is dependent on acidic conditions. Biochim Biophys Acta 1768:2667-80.
32. Mason AJ, Moussaoui W, Abdelrahman T, Boukhari A, Bertani P, Marquette A, Shooshtarizaheh P, Moulay G, Boehm N, Guerold B, Sawers RJ, Kichler A, Metz-Boutigue MH, Candolfi E, Prevost G, Bechinger B. 2009. Structural determinants of antimicrobial and antiplasmodial activity and selectivity in histidine-rich amphipathic cationic peptides. J Biol Chem 284:119-33.
33. Pasupuleti M, Schmidtchen A, Malmsten M. 2012. Antimicrobial peptides: key components of the innate immune system. Crit Rev Biotechnol 32:143-71.

574 34. Huarte N, Carravilla P, Cruz A, Lorizate M, Nieto-Garai JA, Krausslich HG, Perez-Gil J,
575 Requejo-Isidro J, Nieva JL. 2016. Functional organization of the HIV lipid envelope. Sci Rep
576 6:34190.
577 35. Brugger B, Glass B, Haberkant P, Leibrecht I, Wieland FT, Krausslich HG. 2006. The HIV
578 lipidome: a raft with an unusual composition. Proc Natl Acad Sci U S A 103:2641-6.
579 36. Pasha Q, Malik SA, Shah MH. 2008. Statistical analysis of trace metals in the plasma of
580 cancer patients versus controls. J Hazard Mater 153:1215-21.
581 37. Thulin A, Ringvall M, Dimberg A, Karehed K, Vaisanen T, Vaisanen MR, Hamad O, Wang J,
582 Bjerkvig R, Nilsson B, Pihlajaniemi T, Akerud H, Pietras K, Jahnen-Dechent W, Siegbahn A, Olsson
583 AK. 2009. Activated platelets provide a functional microenvironment for the antiangiogenic
584 fragment of histidine-rich glycoprotein. Mol Cancer Res 7:1792-802.
585 38. Mohan KV, Rao SS, Atreya CD. 2010. Antiviral activity of selected antimicrobial peptides
586 against vaccinia virus. Antiviral Res 86:306-11.
587 39. Yeaman MR. 2014. Platelets: at the nexus of antimicrobial defence. Nat Rev Microbiol
588 12:426-37.
589 40. Ceballos A, Remes Lenicov F, Sabatte J, Rodriguez Rodrigues C, Cabrini M, Jancic C, Raiden
590 S, Donaldson M, Agustin Pasqualini R, Jr., Marin-Briggiler C, Vazquez-Levin M, Capani F, Amigorena
591 S, Geffner J. 2009. Spermatozoa capture HIV-1 through heparan sulfate and efficiently transmit the
592 virus to dendritic cells. J Exp Med 206:2717-33.
593 41. Linde ME, Colquhoun DR, Ubaida Mohien C, Kole T, Aquino V, Cotter R, Edwards N,
594 Hildreth JE, Graham DR. 2013. The conserved set of host proteins incorporated into HIV-1 virions
595 suggests a common egress pathway in multiple cell types. J Proteome Res 12:2045-54.
596 42. Tremblay MJ, Fortin JF, Cantin R. 1998. The acquisition of host-encoded proteins by
597 nascent HIV-1. Immunol Today 19:346-51.
598 43. Coombe DR, Kett WC. 2005. Heparan sulfate-protein interactions: therapeutic potential
599 through structure-function insights. Cell Mol Life Sci 62:410-24.
600 44. Wu C, Wang S. 2012. A pH-sensitive heparin-binding sequence from Baculovirus gp64
601 protein is important for binding to mammalian cells but not to Sf9 insect cells. J Virol 86:484-91.
602 45. Norvell MK, Benrubi GI, Thompson RJ. 1984. Investigation of microtrauma after sexual
603 intercourse. J Reprod Med 29:269-71.
604 46. Masters WH, Johnson VE. 1961. The physiology of the vaginal reproductive function. West
605 J Surg Obstet Gynecol 69:105-20.
606 47. Vaughan J, Ngamtrakulpanit L, Pajewski TN, Turner R, Nguyen TA, Smith A, Urban P, Hom
607 S, Gaston B, Hunt J. 2003. Exhaled breath condensate pH is a robust and reproducible assay of
608 airway acidity. Eur Respir J 22:889-94.
609 48. Reid G, Bruce AW. 1995. Low vaginal pH and urinary-tract infection. Lancet 346:1704.
610 49. Fallingborg J. 1999. Intraluminal pH of the human gastrointestinal tract. Dan Med Bull
611 46:183-96.
612 50. Hunt JF, Fang K, Malik R, Snyder A, Malhotra N, Platts-Mills TA, Gaston B. 2000.
613 Endogenous airway acidification. Implications for asthma pathophysiology. Am J Respir Crit Care
614 Med 161:694-9.
615 51. Ricciardolo FL, Gaston B, Hunt J. 2004. Acid stress in the pathology of asthma. J Allergy Clin
616 Immunol 113:610-9.
617 52. Rhodes J, Apsimon HT, Lawrie JH. 1966. pH of the contents of the duodenal bulb in relation
618 to duodenal ulcer. Gut 7:502-8.
619 53. Rune SJ, Viskum K. 1969. Duodenal pH values in normal controls and in patients with
620 duodenal ulcer. Gut 10:569-71.

621 54. Ovesen L, Bendtsen F, Tage-Jensen U, Pedersen NT, Gram BR, Rune SJ. 1986. Intraluminal
622 pH in the stomach, duodenum, and proximal jejunum in normal subjects and patients with
623 exocrine pancreatic insufficiency. Gastroenterology 90:958-62.
624 55. Schmid-Wendtner MH, Korting HC. 2006. The pH of the skin surface and its impact on the
625 barrier function. Skin Pharmacol Physiol 19:296-302.
626 56. Ali SM, Yosipovitch G. 2013. Skin pH: from basic science to basic skin care. Acta Derm
627 Venereol 93:261-7.
628 57. Manderson GA, Martin M, Onnerfjord P, Saxne T, Schmidtchen A, Mollnes TE, Heinegard
629 D, Blom AM. 2009. Interactions of histidine-rich glycoprotein with immunoglobulins and proteins
630 of the complement system. Mol Immunol 46:3388-98.
631 58. Adachi A, Gendelman HE, Koenig S, Folks T, Willey R, Rabson A, Martin MA. 1986.
632 Production of acquired immunodeficiency syndrome-associated retrovirus in human and
633 nonhuman cells transfected with an infectious molecular clone. J Virol 59:284-91.
634 59. Chen C, Okayama H. 1987. High-efficiency transformation of mammalian cells by plasmid
635 DNA. Mol Cell Biol 7:2745-52.
636 60. Popovic M, Sarngadharan MG, Read E, Gallo RC. 1984. Detection, isolation, and continuous
637 production of cytopathic retroviruses (HTLV-III) from patients with AIDS and pre-AIDS. Science
638 224:497-500.
639 61. Blaho JA, Morton ER, Yedowitz JC. 2005. Herpes simplex virus: propagation, quantification,
640 and storage. Curr Protoc Microbiol Chapter 14:Unit 14E 1.

641

642

643 # Figure legends.

644 **Figure 1:** ***HRG inhibits HIV-1 infection at low pH values.*** **A-C.** HIV-1 infection was
645 assessed using the reporter cell line GHOST transfected with CD4, CXCR4 and CCR5
646 genes. Cells were challenged with HIV-1_{IIIB} or HIV-1_{BAL} strains (10 ng of p24/well) for 90
647 min at 37ºC, in the absence or presence of HRG (125 µg/ml), at different pH values. Cells
648 were then washed and cultured for 72 h at pH 7.3, and infection was revealed by flow
649 cytometry. **D**. GHOST cells were challenged with HIV-1_{IIIB} (10 ng of p24/well) for 90 min
650 at 37ºC at pH 7.3 or 6.0, in the absence or presence of different concentrations of HRG.
651 Cells were then washed and cultured for 72 h at pH 7.3, and infection was revealed by flow
652 cytometry. **E** and **F**. Jurkat cells were challenged with HIV-1 NL4-3-EGFP (10 ng of
653 p24/well) for 90 min at 37ºC, in the absence or presence of plasma purified (**E**) or
654 recombinant HRG (125 µg/ml) (**F**), at different pH values. Cells were then washed and
655 cultured for 3 or 5 days at pH 7.3, and infection was revealed by flow cytometry. (**G**) Jurkat
656 cells were challenged with HIV-1 NL4-3-EGFP (10 ng of p24/well) for 90 min at 37ºC, in
657 the absence or presence of different concentrations of plasma purified HRG, at pH 7.3 or
658 6.0. Cells were then washed and cultured for 5 days at pH 7.3, and infection was revealed
659 by flow cytometry. **H.** Monocyte-derived macrophages were challenged with HIV-1_{BAL} (50
660 ng of p24/well) for 90 min at 37ºC, in the absence or presence of HRG (125 µg/ml), at
661 different pH values. Cells were then washed and cultured for 10 days at pH 7.3. Infection
662 was then revealed by intracelular staining of p24 antigen with the mAb Kc-57 and flow
663 cytometry. **I.** Purified CD4+ T cells were activated for 3 days with anti-CD3/CD28 coated
664 beads in the presence of IL-2 (10 U/ml). Cells were challenged with HIV-1 NL4-3-EGFP
665 (50 ng of p24/well) for 90 min at 37ºC in the absence or presence of HRG (125 µg/ml), at
666 different pH values. Then, cells were washed and cultured for 6 days at pH 7.3, and
667 infection was revealed by flow cytometry. **A, D** and **G**: representative experiments (n=4-8)
668 are shown. **B**, **C**, **E** and **F-I**: results are expressed as the mean ± SEM of 4-8 experiments.
669 *$p < 0.01$ vs cells incubated without HRG.

670

Figure 2. HRG is expressed at the female reproductive tract and binds to cells in a pH-dependent manner. (**A**). HRG expression was studied by immunohistochemistry in the female reproductive tract and anal canal. The squamocolumnar junction of the cervix, the ectocervix**,** the vagina and the anal canal show an intense staining for HRG in the basal/parabasal cell layers of the epithelium. A diffuse cytoplasmic staining was observed in the liver. **C** and **D**. Ect1/E6E7 cells, CD4+ T cells previously activated during 3 days with anti-CD3/CD28 coated beads, and macrophages were incubated with HRG (125 µg/ml) at different pH values for 1 hour at 4ºC, and the binding of HRG to the cell surface was then evaluated by flow cytometry. **C** and **D**. Representative experiments are shown (n = 3). *p < 0.01 vs cells incubated without HRG.

Figure 3. ***HRG inhibits early cellular events associated with HIV-1 infection.*** Experiments were performed by incubating (90 min at 37°C) Ect1/E6E7 cells (**A**), VK2/E6E7 cells (**B**), anti-CD3/anti-CD28 activated CD4+ T cells (**C**), macrophages (**D**), Jurkat (**E**) and GHOST cells (**F**), with NL4-3 HIV-1 (50 ng of p24/well), at different pH values, in the absence or presence of HRG (125 µg/ml). Then, cells were extensively washed and lysed using RIPA lysis buffer and the concentration of p24 was evaluated by ELISA as absorbance at 450 nm. **G.** Jurkat cells were incubated for 90 min at 37°C or 4ºC with NL4-3 HIV-1 (50 ng of p24/well), at different pH values, in the absence or presence of HRG (125 µg/ml). Then, cells were extensively washed and lysed using RIPA lysis buffer and the concentration of p24 was evaluated by ELISA as absorbance at 450 nm. Results are expressed as the mean ± SEM of 4-5 experiments. *p < 0.01 vs cell incubated without HRG.

Figure 4. ***Analysis of the mechanisms through which HRG inhibits HIV-1 infection.*** **(A)** GHOST cells were grown during three days in control medium or in sulfate free medium supplemented with sodium chlorate (25mM) (**left**) or treated with heparinases I, II, and III (5 mIU/ml) during 90 min at 37°C (**right**). Then, the expression of HS was evaluated by flow cytometry. (**B)** GHOST cells were treated as described in (**A**). Then,

700 HRG binding assays were performed by incubating cells with HRG (125 µg/ml) at pH 7.3
701 or 6.0, for 60 min at 4ºC. HRG binding was then revealed by flow cytometry. (**C**) Untreated
702 (controls) or heparinase-treated Jurkat cells were incubated for 90 min at 37°C with NL4-3
703 HIV-1 (50 ng of p24/well), at different pH values, in the absence or presence of HRG (125
704 µg/ml). Then, cells were extensively washed and lysed using RIPA lysis buffer and the
705 concentration of p24 was evaluated by ELISA as absorbance at 450 nm. **(D)** Untreated or
706 heparinase-treated Jurkat cells were challenged with HIV-1 NL4-3-EGFP (10 ng of
707 p24/well) for 90 min at 37ºC, in the absence or presence of HRG (125 µg/ml), at pH 7.3 or
708 6.0. Cells were then washed, and infection was revealed by flow cytometry after 5 days of
709 culture at pH 7.3. **E and F.** GHOST cells were treated as described in (**A**). Then, cells were
710 challenged with HIV-1 NL4-3 (10 ng of p24/well) for 90 min at 37°C, at pH 7.3 or 6.0, in
711 the absence or presence of HRG (125 µg/ml). Cells were then washed and cultured for 72 h
712 at pH 7.3, and infection was revealed by flow cytometry. (**G)** HIV-1 NL4-3 (50 ng of
713 p24/well) was preincubated, or not, with 125µg/ml of HRG at pH 7.3 or 6.0, for 90 min at
714 37°C. After this period, the viral suspension was centrifuged twice to wash out HRG, and
715 resuspended in culture medium at pH 7.3 or pH 6.0, respectively. Then, Jurkat cells were
716 exposed to these viral suspensions for 90 min at 4°C, washed, lysed with RIPA lysing
717 buffer, and the amount of p24 antigen was evaluated by ELISA as absorbance at 450 nm.
718 (**H)**. HIV-1 NL4-3-EGFP (10 ng of p24/well) was preincubated, or not, with 125µg/ml of
719 HRG at pH 7.3 or 6.0, for 90 min at 37°C. After this period, the viral suspension was
720 centrifuged twice to wash out HRG, and resuspended in culture medium at pH 7.3 or pH
721 6.0, respectively. Then, Jurkat cells were exposed to these viral suspensions for 90 min at
722 37°C, at pH 7.3 or 6.0. Cells were washed, and cultured for 3 days at pH 7.3, and infection
723 was revealed by flow cytometry. Representative experiments (n = 3) are shown in (**A**) and
724 (**B**). In **C**-**H**, results are expressed as the mean ± SEM of 3-5 experiments. *p < 0.01,
725 control vs HRG.
726

727 **Figure 5.** ***Low pH enables HRG to interact with HIV-1.*** **A, left.** HRG-coated latex beads
728 were analyzed by flow cytometry using a mouse IgG mAb anti-HRG and a FITC-IgG anti-
729 mouse IgG. BSA-coated latex beads were used as controls. **A, right.** Latex beads coated

with BSA or the anti-gp120 mAb 2G12, were incubated for 45 min at 37°C under agitation with HIV-1 NL4-3 Gag-iGFP virus (10 ng of p24), at pH 7.3 or 6.0. Then, HIV-1 capture by latex beads was analyzed by flow cytometry. **B and C**. Latex beads coated with BSA, nonspecific IgG, purified HRG or recombinant HRG, were incubated for 45 min at 37°C under agitation with HIV-1 NL4-3 Gag-iGFP virus (10 ng of p24), at pH 7.3 or 6.0. Then, HIV-1 capture by latex beads was analyzed by flow cytometry. When indicated, heparin (50 U/ml) was added during the capture assay. In experiments directed to analyze the reversibility of HIV-1 association with HRG, latex beads coated with purified HRG were incubated for 45 min at 37°C with HIV-1 NL4-3 Gag-iGFP virus (10 ng of p24) at pH 6.0. Then, the pH was corrected, or not, to 7.3, and the beads was incubated for an additional period of 45 min at 37°C. Then, HIV-1 capture by latex beads was analyzed by flow cytometry. Representative experiments (n = 3-5) are shown.

Figure 6. HRG exerts an irreversible deleterious effect on the viral particles. (**A)** HIV-1 NL4-3-EGFP (10 ng of p24/well) was preincubated, or not, with 125µg/ml of HRG at pH 7.3 or 6.0, for 90 min at 37°C. After this period, the viral suspension cultured with HRG at pH 6.0 was neutralized back to pH 7.3. Then, Jurkat cells were exposed to these viral suspensions for 90 min at 4°C, washed, lysed with RIPA lysing buffer, and the amount of p24 antigen was evaluated by ELISA as absorbance at 450 nm. (**B)** HIV-1 NL4-3-EGFP (10 ng of p24/well) was preincubated, or not, with 125µg/ml of HRG at pH 7.3 or 6.0, for 90 min at 37°C. After this period, the viral suspension cultured with HRG at pH 6.0 was neutralized back to pH 7.3. Then, Jurkat cells were exposed to these viral suspensions for 90 min at 37°C, at pH 7.3. Cells were washed, and cultured for 3 days at pH 7.3, and infection was revealed by flow cytometry. (**C)** HIV-1 NL4-3-EGFP (10 ng of p24/well) was preincubated, or not, with 125µg/ml of HRG at pH 6.0, for 90 min at 37°C. Then, the pH was neutralized back to pH 7.3, and Jurkat cells were exposed to these viral suspensions for 90 min at 37°C and pH 7.3, immediately or after further incubation at pH 7.3 of the viral suspensions for 90 min and 180 min. Then, cells were washed, and cultured for 3 days at pH 7.3, and the infection was revealed by flow cytometry. Results are expressed as the mean ± SEM of 4-5 experiments. *$p < 0.01$ vs cell incubated without HRG.

Figure 7. Low pH enables HRG to display a broad antiviral activity. (A) Jurkat cells were challenged with VSV-G pseudotyped NL4-3 ΔEnv-EGFP (10 ng p24/well) for 90 min at 37ºC, in the absence or presence of HRG (125 µg/ml), at different pH values. Cells were then washed, cultured for 5 days at pH 7.3, and infection was revealed by flow cytometry. (**B).** Hep-2 cells (~50% confluence) were challenged with a pre-titered amount of RSV for 90 min at 37°C, in the absence or presence of HRG (125 µg/ml), at different pH values. Cells were then washed, cultured for 3 days at pH 7.3, and infection was revealed by flow cytometry. **C**. Vero cells (~80% confluence) were challenged with a pre-titered of HSV-2 for 90 min at 37°C, in the absence or presence of HRG (125 µg/ml), at different pH values. Cells were then washed, cultured for 3 days at pH 7.3, and infection was evaluated by determining the number of pfu/well. **D-F** Ect1/E6E7 (**D**), VK2/E6E7 (**E**) and HeLa cells (**F**)(~80% confluence) were challenged with a pre-titered amount of HSV-1 derived amplicon vector encoding GFP, in the presence or absence of HRG (125 µg/ml), for 90 min at 37°C, at different pH values. Then, cells were washed, cultured for 3 days at pH 7.3, and infection was revealed by flow cytometry. Results are expressed as the mean ± SEM of 3-4 experiments. *$p < 0.01$ vs cell incubated without HRG.

Figure 1

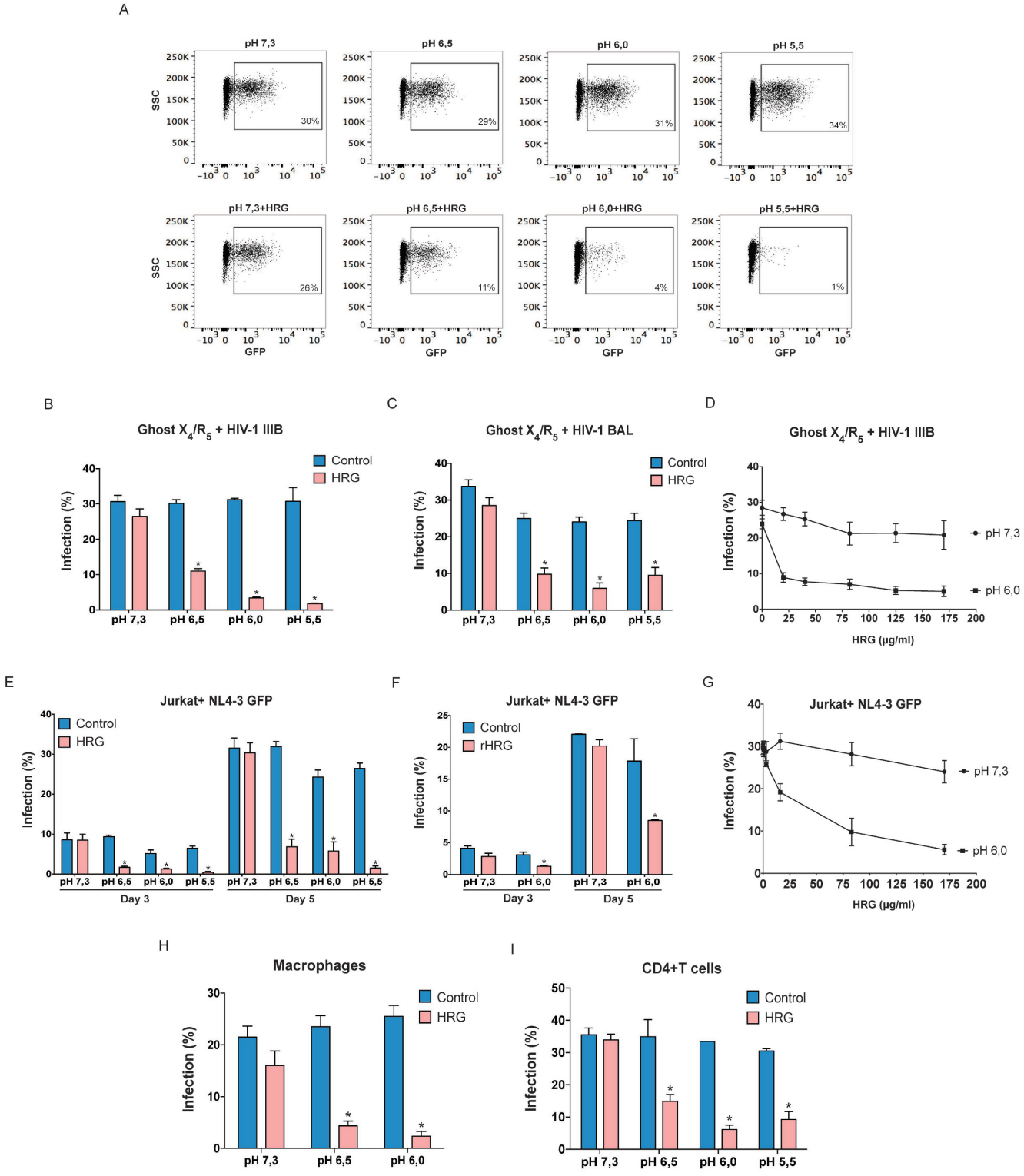

Figure 2

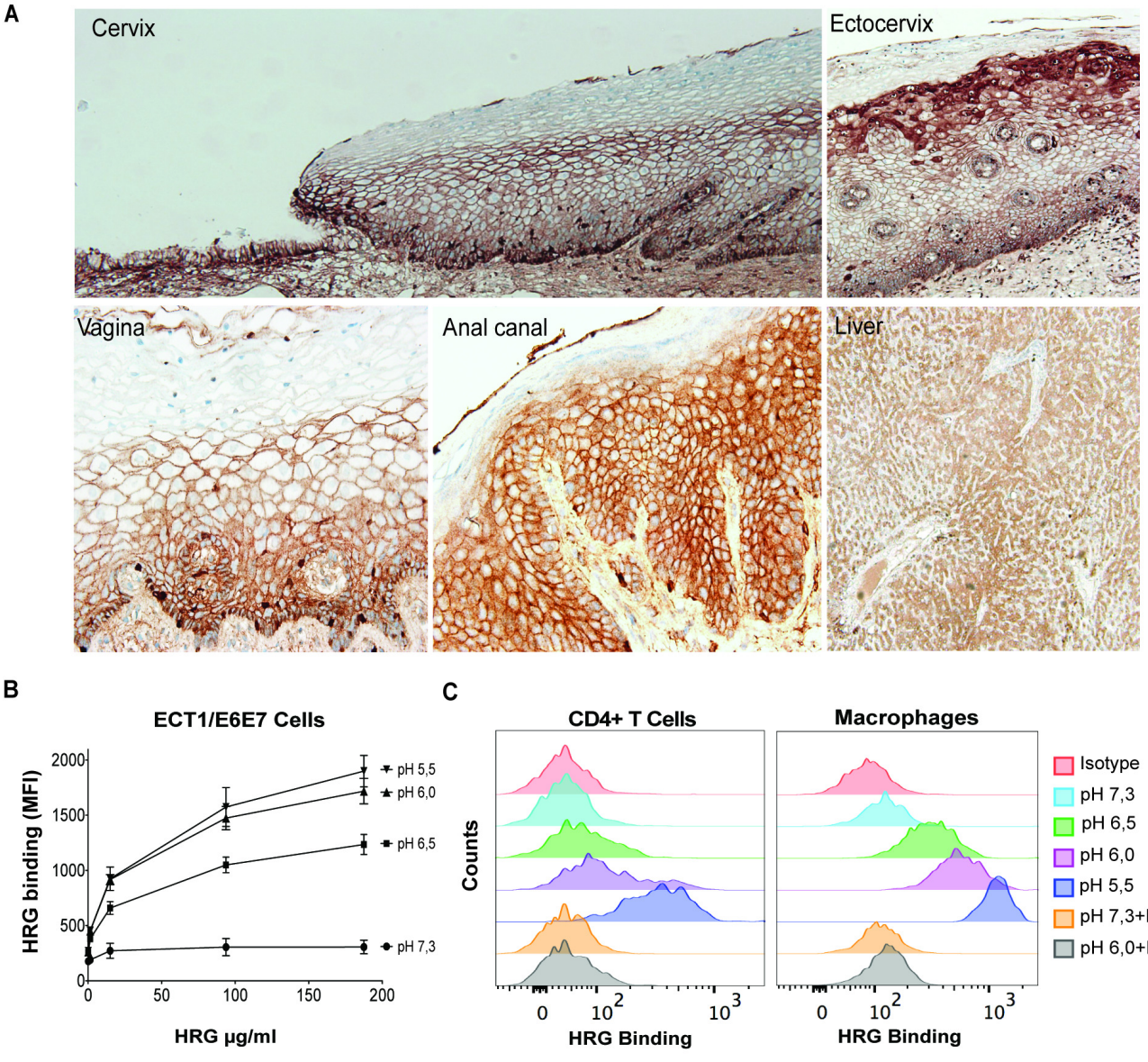

Figure 3

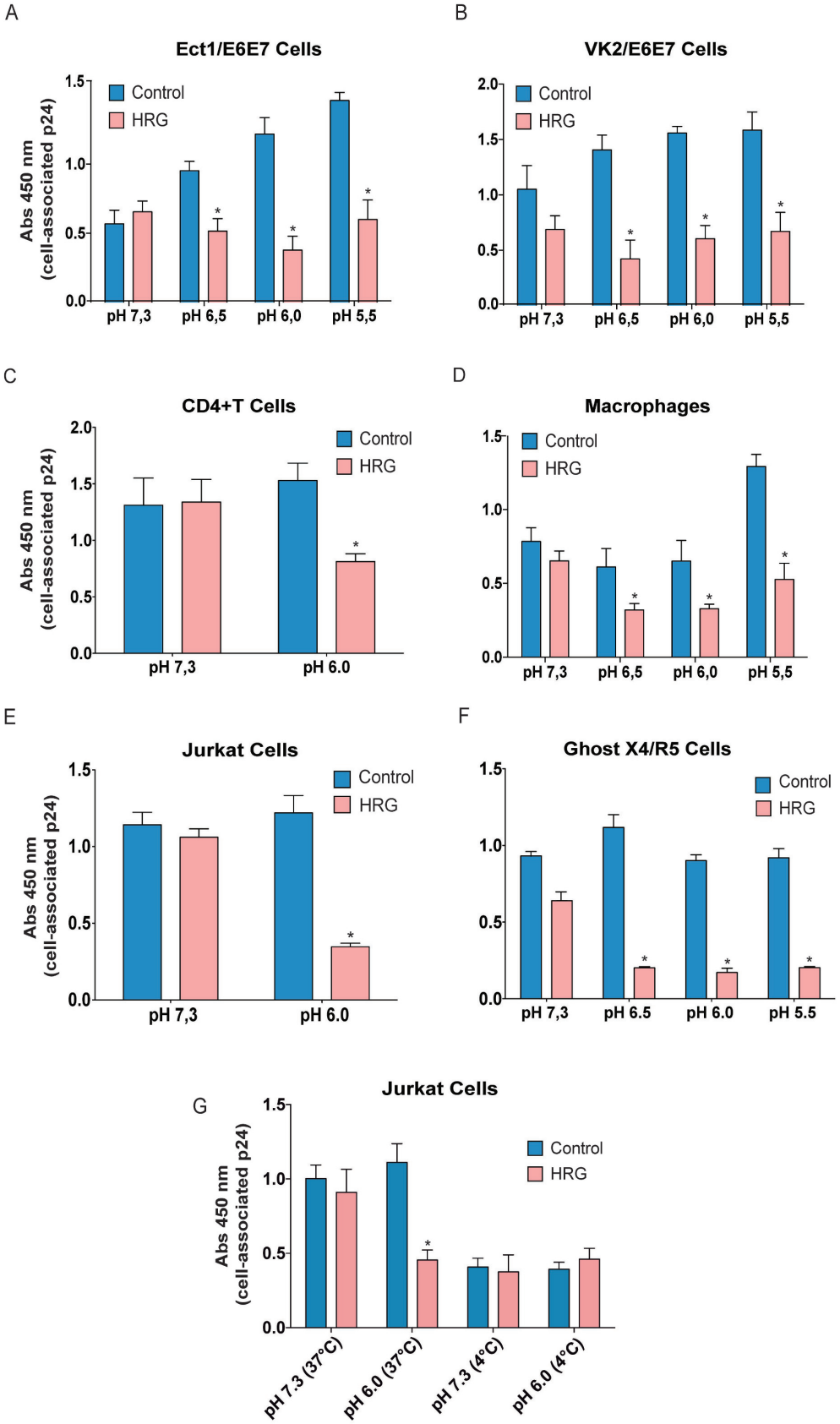

Figure 4

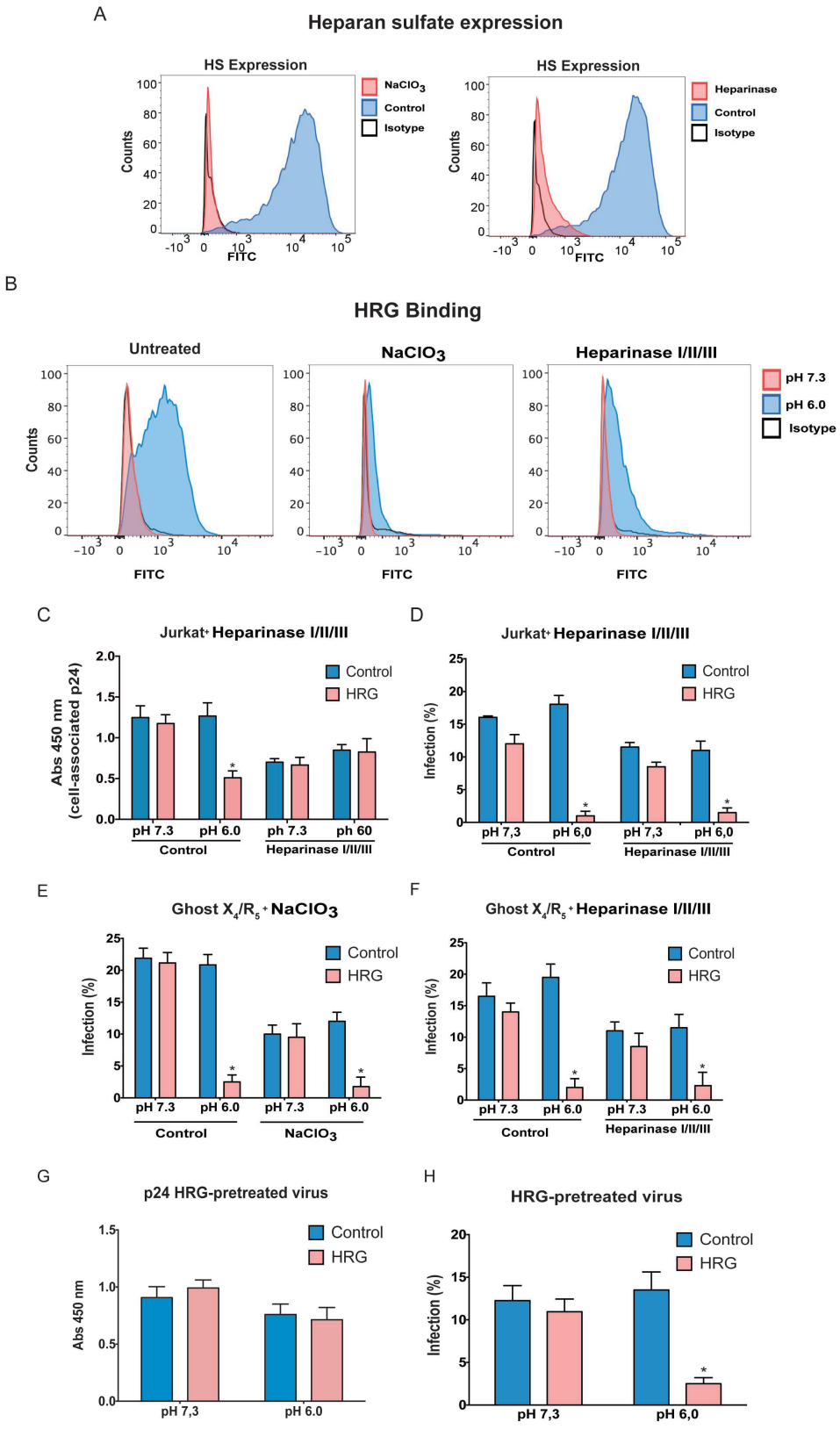

Figure 5

A

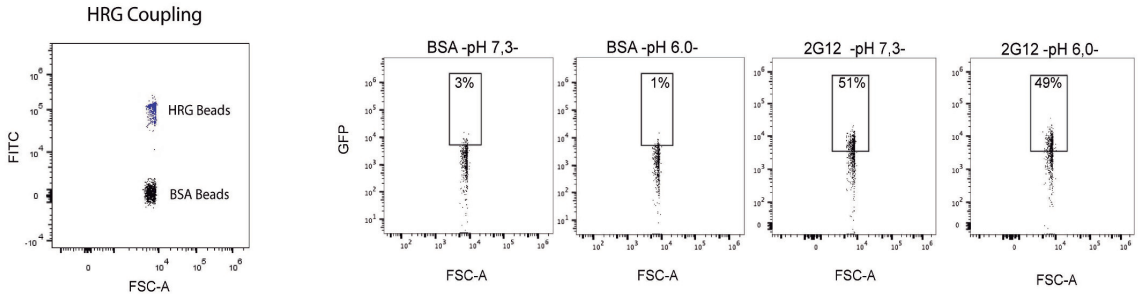

B

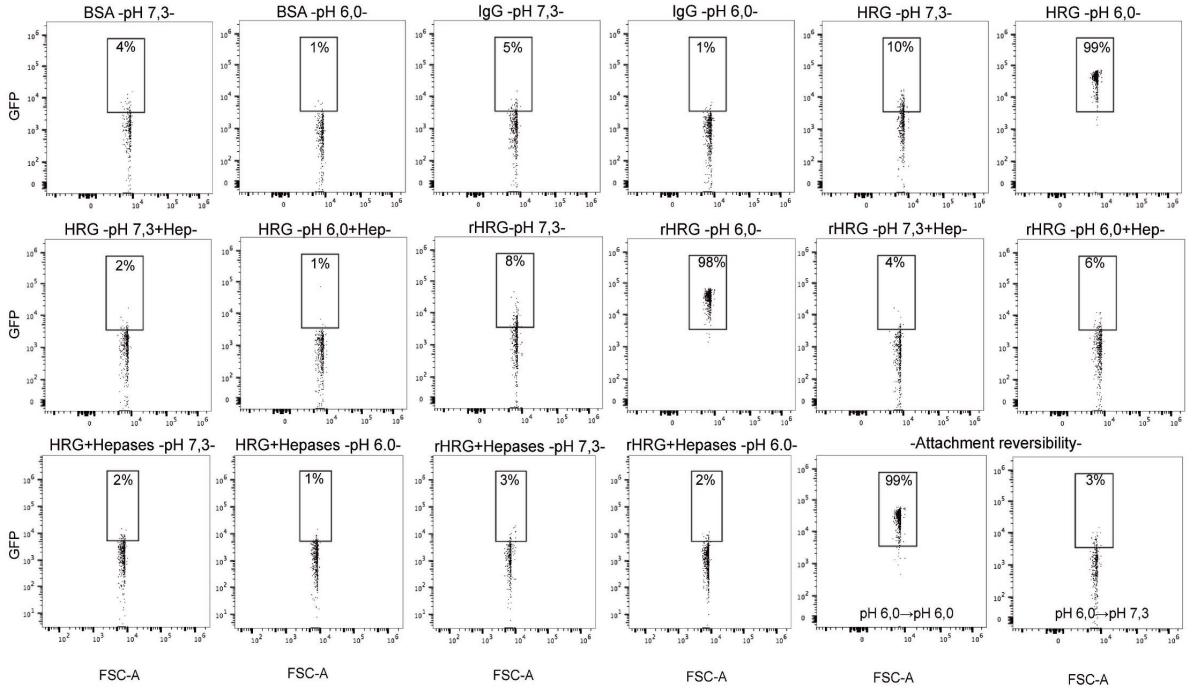

C

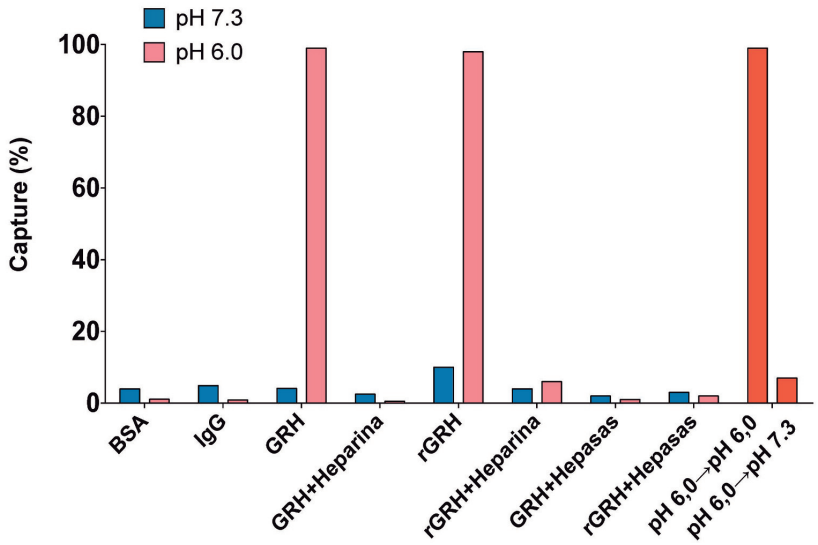

Figure 6

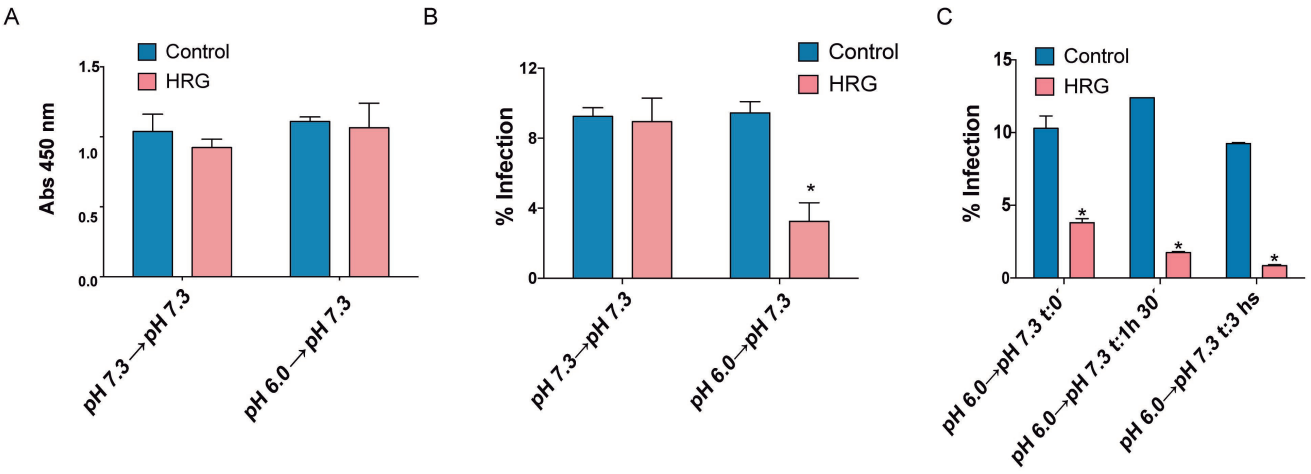

Figure 7